Application of Photoelectron Spectroscopy to Molecular Properties. Part 19.[1] Electronic Structure of Tris(α-di-imino) Complexes of Ruthenium(0) †

Claude Guimon and Geneviève Pfister-Guillouzo *
Laboratoire de Physico-Chimie Moléculaire ERA 895, I.U.R.S., Avenue L. Sallenave, 64000 Pau, France
Bruno Chaudret and René Poilblanc
Laboratoire de Chimie de Coordination du C.N.R.S. associé à l'Université Paul Sabatier, 205 route de Narbonne, 31400 Toulouse, France

A study of the electronic structure of the formally 20-electron complex tris[1,2-bis(*p*-methoxyphenylimino)-ethane]ruthenium(0) is described using multiple scattering MSXα calculations coupled with He(I) photoelectron as well as visible and u.v. spectroscopy. This study shows a very low energy gap between the highest occupied molecular orbital and the lowest unoccupied molecular orbital of the complex; both are localized on the ligand, which explains its magnetic behaviour.

The structure and properties (magnetic, chemical, and photochemical) of Group 8 metal chelate complexes exhibiting a d^6 configuration (Fe^{II}, Ru^{II}, and Os^{II})[2] have been widely studied for the past few years. Most tris(α-di-imino) complexes of these metals are of great interest when considering energy transfers and especially solar energy conversion[3,4] because of the presence of a metal-to-ligand charge-transfer band in their electronic (visible) spectrum.

The electronic structure of these compounds has been discussed for a long time[5-13] and it now seems well established despite the small number of quantum studies.[14,15]

Recently, we prepared[16,17] a similar complex (neutral and richer in electrons: 20 instead of 18), tris[1,2-bis(*p*-methoxyphenylimino)ethane]ruthenium(0), $[Ru(bmpie)_3]$. This compound is diamagnetic at −80 °C and weakly paramagnetic at room temperature. It seemed interesting to study the origin of this rather rare property. Therefore we analysed the electronic structure of the complex using the MSXα method coupled to experimental techniques such as He(I) u.v. photoelectron spectroscopy and u.v. and visible electronic spectroscopy.

Results and Discussion

Methods of Calculation.—The standard version of the 'multiple scattering MSXα method'[18-20] was used. An atomic sphere overlap of 25% was allowed between adjacent carbon atoms as well as betweeen carbon and nitrogen atoms. An overlap of 30% was allowed between carbon or nitrogen and hydrogen atoms, and finally an overlap of 8% between the metal (ruthenium) and nitrogen. All the parameters used are shown in Table 1. The geometry used for this calculation was obtained from an *X*-ray diffraction study on the tris(α-di-imino) complex $[Ru(bmpie)_3]$ in which *p*-methoxyphenyl groups are bound to nitrogen. Due to problems of calculation time and program capacity, the theoretical model is the unsubstituted molecule HN=CHCH=NH.

In order to facilitate the analysis of the interactions between the atomic orbitals of ruthenium (4*d*, 5*s*, 5*p*) and the molecular orbitals of the ligands, we used the EHT-FMO method (extended Hückel technique[21-24] and fragment molecular orbital[25]).

Finally, the experimental attribution of the photoelectron spectra of the α-di-imine ligand was compared to the results of MNDO (modified neglect of diatomic overlap) calculations[26] which were run with a minimization of the total energy as a function of geometric parameters.

Table 1. MSXα parameters for $[Ru(bmpie)_3]$. The values corresponding to the *cis*-di-imine are given in parentheses

Atom	Sphere radius (R_y)	α *	$l_{max.}$
Ru	2.650 50	0.702 53	2
N	1.552 92	0.751 97	1 (1)
C	1.624 20	0.759 28	1 (1)
H (NH)	0.928 30	0.777 25	0 (0)
H (CH)	1.053 55	0.777 25	0 (0)
Outer sphere	8.534 20	0.763 88	4 (2)

* See K. Schwarz, *Phys. Rev., Ser. B*, 1972, **5**, 2466; *Theor. Chim. Acta*, 1974, **34**, 225.

Table 2. Calculated ionization potentials ($i.p._{calc.}$/eV)[a] of MeN=CHCH=NMe in its *trans* and *cis* forms and experimental values ($i.p._{exp}$/eV) for its isopropyl homologue[b]

MeN=CHCH=NMe		$Pr^iN=CHCH=NPr^i$
trans	*cis*	
10.54 (^2A_g)	10.39 ($^2A_1$)	
10.76 (^2A_u)	10.61 ($^2A_2$)	9.0—9.6
10.99 (^2B_u)	10.66 ($^2B_2$)	
12.41 (^2B_g)	12.28 ($^2B_1$)	11.3

[a] MNDO method[26] within the framework of Koopmans' approximation (T. Koopmans, *Physica*, 1934, **1**, 34). [b] From H. T. Dieck, K. D. Franz, and W. Majunke, *Z. Naturforsch., Teil B*, 1975, **30**, 922.

Electronic Structure of 1,2-*Bis*(p-*methoxyphenylimino*)-*ethane.*—The molecular orbitals of this ligand (bmpie) are easily deduced from those localized on the di-imino fragment and on the *p*-methoxyphenyl groups. Figure 1 gives the ionization potentials related to the orbitals of the ligand as well as to several diazadienes. The two orbitals n_N and $\pi_{C=N}$ of the imine are split into bonding (n^+, π^+) and antibonding (n^-, π^-) combinations in the di-imine and thus give four orbitals of symmetry a_u (π^-), a_g (n^+), b_u (n^-), and b_g (π^+) if the molecule is considered in its *trans* configuration (C_{2h} symmetry). When only nitrogen atoms are substituted, the three a_u, a_g, and b_u orbitals are virtually degenerate and correspond to a single somewhat broad band in the photoelectron spectrum (see Table 2). When replacing isopropyl groups by aromatic rings, four new ionization potentials are seen in the

---

† *Non-S.I. unit employed*: eV ≈ 1.60 × 10^{-19} J.

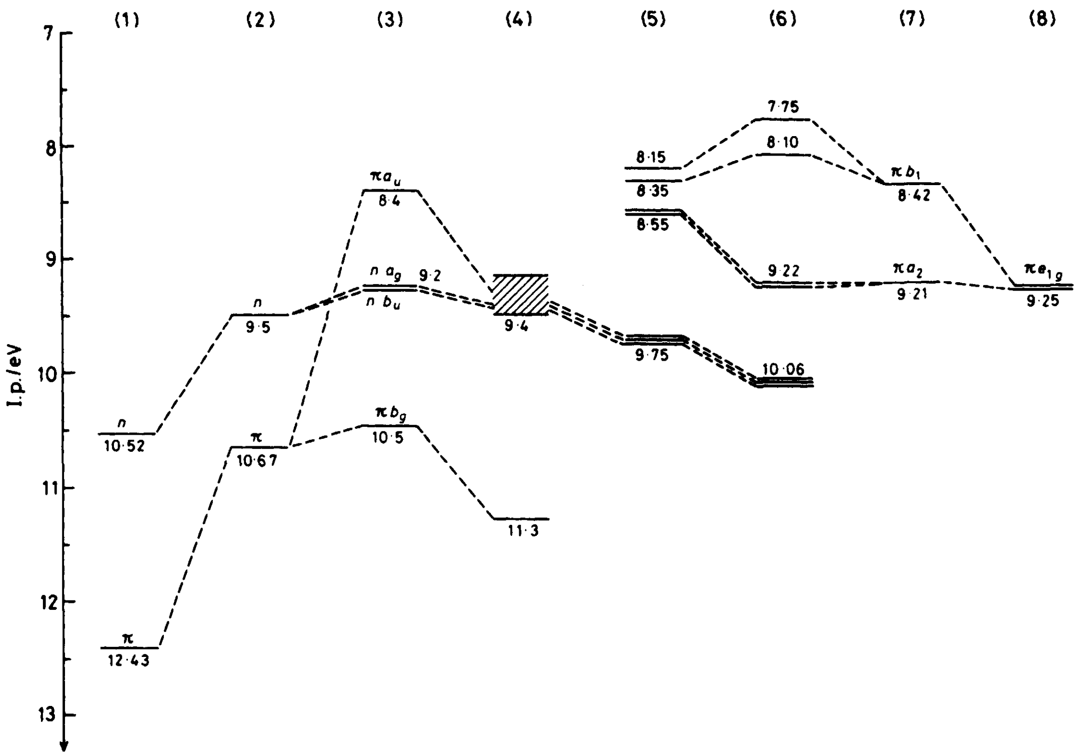

Figure 1. Ionization potentials and assignments of some α-di-imines. (1) $H_2C{=}NH$ (ref. 27); (2) MeHC=NH (J. B. Peel and G. D. Willet, *J. Chem. Soc., Faraday Trans. 2*, 1975, 1799); (3) $Pr^iN{=}CMeCMe{=}NPr^i$ (E. Haselbach and E. Heilbronner, *Helv. Chim. Acta*, 1970, **53**, 684); (4) $Pr^iN{=}CHCH{=}NPr^i$ (see previous ref.); (5) $2,6\text{-}Pr^i{}_2C_6H_3N{=}CHCH{=}NC_6H_3Pr^i{}_2\text{-}2,6$; (6) bmpie; (7) C_6H_5OMe (H. T. Dieck, K. D. Franz, and W. Majunke, *Z. Naturforsch., Teil B*, 1975, **30**, 922); (8) C_6H_6 (J. P. Maier and D. W. Turner, *J. Chem. Soc., Faraday Trans.* 2, 1973, 521). (1), (2), (7), and (8) help to assign the ionization potentials of the α-di-imines

Table 3. Overlaps (EHT calculation) between 4*d* a.o.s of ruthenium and frontier orbitals of the di-imine fragment bmpie whose C_2 symmetry axis is 0_y

	Ru				
bmpie	$d_{x^2-y^2}$	d_{z^2}	d_{xy}	d_{xz}	d_{yz}
$2a_2$	0.011	−0.020		0.008	
$2b_1$			0.035		−0.025
$1a_2$	0.027	−0.046		0.019	
$4b_2$			0.100		0.141
$5a_1$	0.062	0.016		−0.482	
$1b_1$			−0.052		0.037

low-potential area (less than 10 eV); they are due to the ionization of orbitals localized on these rings. MNDO calculations (see Table 2) are in good agreement with the attributions deduced from the comparison between the different spectra (see Figures 1 and 2). Furthermore they show the weak influence of the conformation (*trans* or *cis*) of the di-imine group; this had already been noticed in the case of butadiene.[27] We thus will be able to compare the ionization potentials of the free ligand (*trans* form) with those of the ligand in the complex (*cis* form).

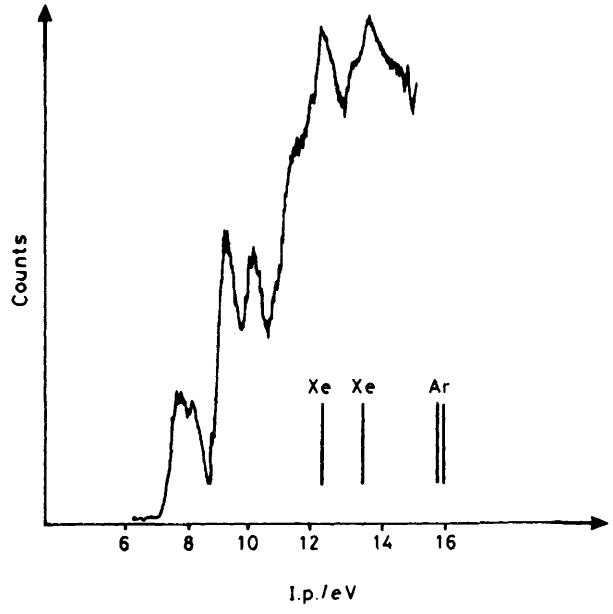

Figure 2. He(I) Photoelectron spectrum of bmpie

Electronic Structure of $[Ru(bmpie)_3]$.—The shape and localization of the molecular orbitals of this compound are a function of the interactions between the orbitals localized on the three diazadiene ligands and the atomic orbitals of ruthenium ($4d^8$, $5s^0$, $5p^0$). In the case of an octahedral environment, the *d* orbitals of the metal are combined in a set of three stable degenerate orbitals, X_1, X_2, X_3, of t_{2g} symmetry, and two less stable orbitals X_4 and X_5 (doubly degenerate), of e_g symmetry. The decrease of symmetry from O_h to D_3 for $[Ru(bmpie)_3]$ allows a partial splitting of the t_{2g} levels to give an a_1 (d_{z^2}) and two *e* orbitals (combination of d_{xy} and d_{yz} for X_1, and of $d_{x^2-y^2}$ and d_{xy} for X_2).* Both X_4 orbitals (d_{yz} + d_{xy},

---

* The 0_z axis is the C_3 axis of symmetry of the complex. The origin 0 is the ruthenium atom. The 0_y axis is the C_2 symmetry axis of a di-imine ligand.

Table 4. MSXα energy levels, m.o. localizations (%), vertical experimental (i.p.$_{\text{exp}}$) and calculated (i.p.$_{\text{calc}}$) ionization potentials of [Ru(bmpie)$_3$]. The values of i.p.$_{\text{calc}}$ are calculated within the transition-state procedure

M.o.	Ru	N	C	H (NH)	H (CH)	Inner	Outer	Energy/eV	I.p.$_{\text{calc}}$/eV	I.p.$_{\text{exp}}$/eV
$14e$	57	26	2	1	1	13	1	−3.74		
$8a_1$	0	4	1	0	0	80	15	−3.86		
$13e$	11	38	22	0	0	28	0	−5.71		
$6a_2$	0	40	26	0	0	33	1	−6.06	8.09	8.0
$7a_1$	59	19	7	0	0	15	0	−8.27	10.32	9.3
$12e$	54	14	14	1	0	17	0	−8.66	10.71	
$11e$	10	47	14	0	0	27	0	−9.78	11.82	11.0
$5a_2$	8	55	9	4	4	20	0	−10.53	12.60	11.5—12.0
$6a_1$	29	38	6	1	0	26	0	−10.68	12.72	
$10e$	17	47	11	4	6	16	0	−11.10	13.17	
$4a_2$	1	32	33	1	0	33	0	−11.61	13.63	

if omitting the normalization coefficients) and X_5 ($d_{xz} - d_{x^2-y^2}$) remain degenerate (e symmetry).

The interactions between the X orbitals and the orbitals localized on the bmpie ligand are a function of their overlap. Their values calculated by the EHT method[21-24] are given in Table 3. The energy (MSXα method), the localization of the frontier orbitals, as well as the calculated and experimental ionization potentials are shown in Table 4. The outlines of the main frontier orbitals in different planes are shown in Figure 3 for a better visualization of the interactions.

The two orbitals X_4 and X_5 are destabilized by their interaction with the combinations of the non-bonding orbitals (lone pairs) localized on the nitrogen atoms and thus give rise to the two degenerate vacant orbitals $14e$. This is clear when looking at Figure 3(a) which corresponds to the mixture of X_4 ($d_{yz} + d_{xy}$) and the $4b_2$ orbital of the di-imine. The other combination, X_5, mainly interacts with the $5a_1$ orbital of the ligand.

The three more stable vacant orbitals have $8a_1$ and $13e$ symmetry. Whereas the $8a_1$ molecular orbital (combination of $2a_2$ orbitals of the ligands) is completely localized on the ligands, both degenerate $13e$ molecular orbitals (m.o.s) appear to be mixtures of the $2b_1$ orbital of the ligands interacting with X_1 and X_2. We give an example in Figure 3(b) * which shows the antibonding interaction between $2b_1$ orbitals and X_1 ($d_{xy} + d_{yz}$).

The highest occupied molecular orbital (h.o.m.o.) $6a_2$ is completely localized on the ligands [almost negligible weight of the $5p$ atomic orbital (a.o.) of ruthenium] and corresponds to the bonding mixture of $2b_1$ orbitals [Figure 3(c)]. This orbital is vacant (lowest unoccupied molecular orbital, l.u.m.o.) in the more classical Ru$^{\text{II}}$ complexes.

The three following orbitals in the order of stability ($7a_1$ and $12e$) are essentially d orbitals. The $7a_1$ orbital comes from X_3 (d_{z^2}) destabilized by occupied π orbitals ($1a_2$) of the di-imine groups [Figure 3(d)]. The $12e$ orbitals originate in the interaction between X_1 and X_2, and the π orbitals $2b_1$ and $1a_2$ (and slightly $1b_1$).

Figure 3(e) shows the mixture of X_1 and of the vacant $2b_1$ orbital of the ligands.

All the above observations have allowed us to build the correlation diagram shown in Figure 4. In contrast to most ruthenium complexes having a d-characterized h.o.m.o., the h.o.m.o. of [Ru(bmpie)$_3$] is entirely localized in the ligands and is built from their l.u.m.o. ($2b_1$). This implies a formal transfer of two electrons from the metal (having four $4d$ a.o.s occupied before complexation and thus three $4d$ occupied after complexation) to the ligands.† Nevertheless this loss of charge is greatly compensated by a ligand-to-metal transfer due to the interaction of the occupied m.o.s of di-imine groups with X_4 and X_5, combinations of the vacant $4d$ orbitals of ruthenium (Figure 3). Table 5 shows the atomic charges on the di-imine bmpie and [Ru(bmpie)$_3$] calculated by the MSXα method. It is remarkable that the nitrogen atom in the complex bears a slight excess negative charge (−0.09 e) when compared with the free ligand; this is due to partial occupation of the vacant $2b_1$ m.o.s of these ligands by complexation (the corresponding $6a_2$ orbital of the complex is thus largely localized on the nitrogen atoms; see Table 4). In contrast, the carbon and hydrogen atoms lose a small charge in the complex as compared to the free ligand (0.03 and 0.05, respectively). This is probably due to interactions between $5a_1$ and $4b_2$ and the X_4 and X_5 combinations ($5a_1$ and $4b_2$ m.o.s are localized in part on the carbon and hydrogen atoms).

Photoelectron Spectrum of [Ru(bmpie)$_3$].—1,2-Bis(p-methoxyphenylimino)ethane shows four first ionization potentials (7.75, 8.10, and two near 9.2 eV) associated with the phenyl rings (Figures 1 and 2) and two resulting from electron loss on the di-imino part of the molecule (10.06 eV). It is likely that the m.o.s localized on aromatic rings are little disturbed by complexation especially since the molecular planes of these cycles are presumably approximately orthogonal to those of the di-imine. In contrast, the m.o.s localized on the di-imine groups must be greatly stabilized because of their interaction with d orbitals of ruthenium (X_4 and X_5). This stabilization is observed in all such complexes and may be estimated to within *ca.* 1 eV (from a p.e.s. study of Worley *et al.*[29] on the cyclobutadiene ligand).

These considerations allow us to propose the following assignment for the spectrum of [Ru(bmpie)$_3$] (see Figure 5).

The first relatively weak band centred at *ca.* 8 eV (between 7.7 and 8.2 eV) probably results partially from the orbitals localized on the aromatic cycles (the corresponding bands

---

* Figure 3(b)—(e) shows m.o.s in the plane $0yz$. Point A represents the intersection of the 0_y axis with the line joining both nitrogen atoms of a di-imine ligand [see Figure 3(a)]. Note that in this plane, the contours drawn on the $z > 0$ side correspond to the portion of space above the molecular plane of the ligand whereas those drawn on the $z < 0$ side correspond to the portion of space under this plane.

† The $2b_1$ m.o.s are bonding for the C–C bond and antibonding for the C=N bond. Their presence among the occupied m.o.s of the complex induces an important shortening of the C–C bond in [Ru(bmpie)$_3$] when compared to the Ru$^{\text{II}}$ complex [Ru(bmpie)$_3$]$^{2+}$ (1.375 [17] and 1.476 Å,[28] respectively).

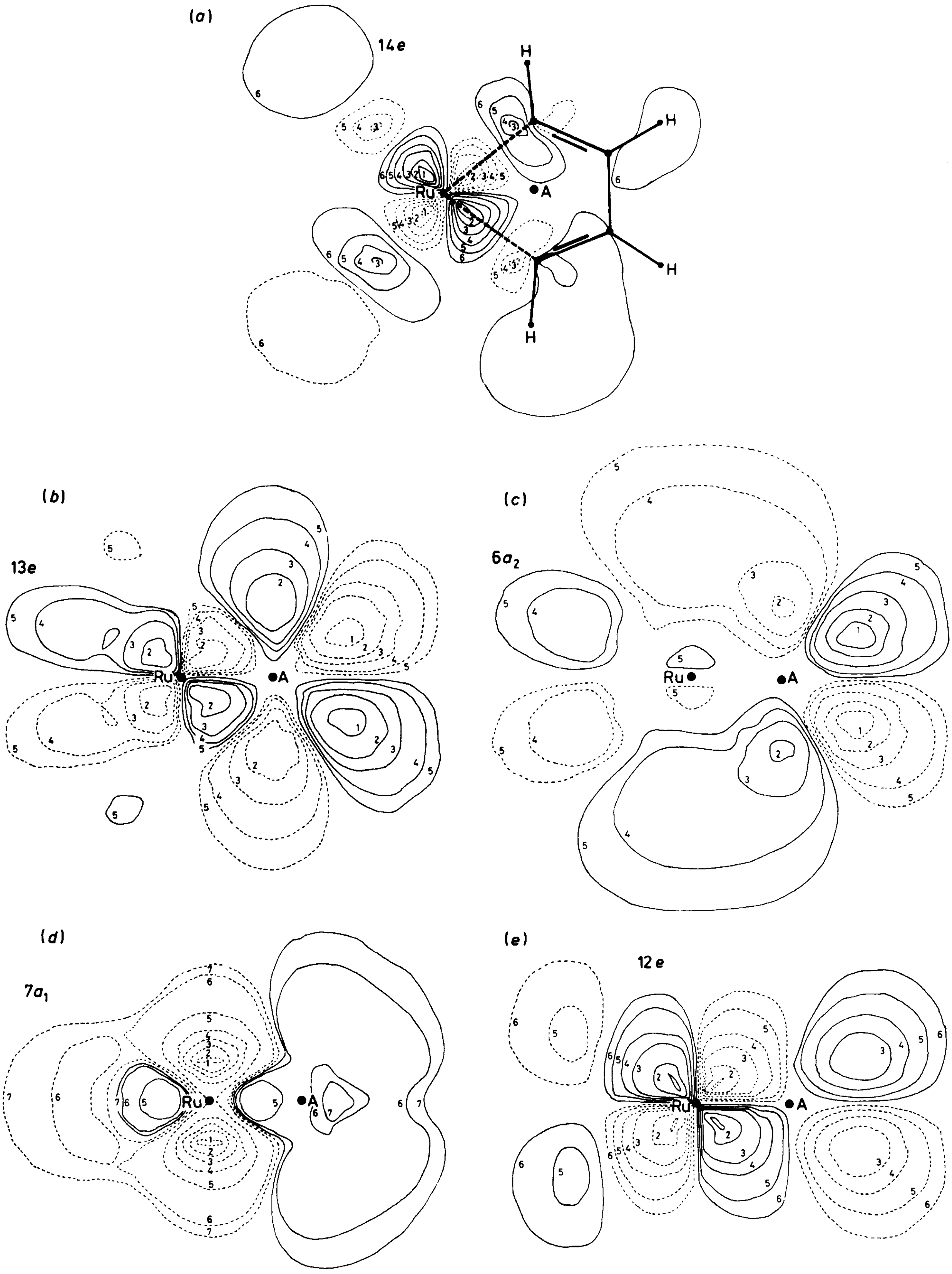

Figure 3. Wavefunction contours. (*a*) The 14*e* m.o. in a ligand plane. Contour values 1, 2, 3, 4, 5, 6 are equal to 0.25, 0.2, 0.15, 0.1, 0.05, 0.01 (electron Bohr^{-3})$^{\frac{1}{2}}$. Here, and in (*b*)—(*e*) the positive wavefunction contours are indicated by solid lines while the negative contours are represented by dashed lines. (*b*) The 13*e* m.o. in the 0*yz* plane [contours are 0.1, 0.05, 0.025, 0.010, 0.005 (electron Bohr^{-3})$^{\frac{1}{2}}$]. (*c*) The 6a_2 m.o. in the 0*yz* plane [contours are 0.075, 0.05, 0.025, 0.01, 0.005 (electron Bohr^{-3})$^{\frac{1}{2}}$]. (*d*) The 7a_1 m.o. in the 0*yz* plane [contours are 0.24, 0.20, 0.15, 0.1, 0.05, 0.01, 0.005 (electron Bohr^{-3})$^{\frac{1}{2}}$]. (*e*) The 12*e* m.o. in the 0*yz* plane [contours are 0.14, 0.10, 0.05, 0.025, 0.010, 0.005 (electron Bohr^{-3})$^{\frac{1}{2}}$]

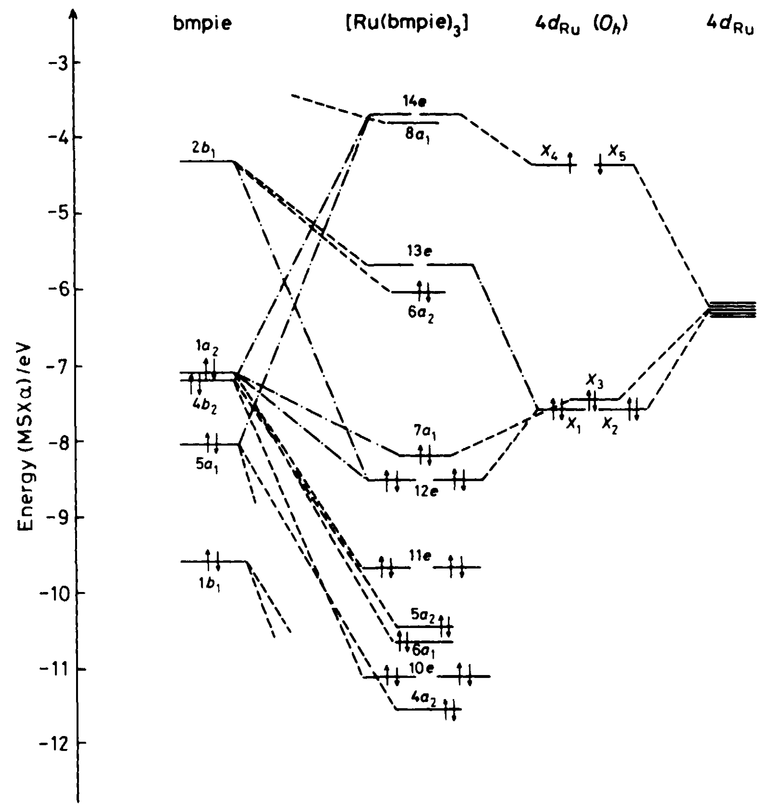

Figure 4. Interaction diagram for [Ru(bmpie)$_3$]

Table 5. MSXα electronic charges (in e) in bmpie and [Ru(bmpie)$_3$]

	Neutral atom	bmpie	[Ru(bmpie)$_3$]
Ru	44		44.18
N	7	7.30	7.39
C	6	6.32	6.29
H (NH)	1	0.61	0.56
H (CH)	1	0.78	0.73

in the free-ligand spectrum at 7.75 and 8.1 eV are also weak, Figure 2) and for the other from the 6a_2 orbital (see above).

The intense peak between 8.9 and 9.6 eV (maximum at 9.25 eV) must be composed of the bands associated with the other orbitals localized on aromatic rings (9.2 eV in the free ligand) and with the three 7a_1 and 12e orbitals having an important d character.

The next peak is even broader and more complex since it lies between 10.8 and 12.3 eV. It shows a first band towards 11 eV related to the 11e orbital, then a more intense band which must be composed of the ionizations of the 5a_2, 6a_1, and 10e orbitals and of the orbitals localized on the aromatic rings and oxygen atoms.

As a whole, the values of the ionization potentials calculated in the formalism of the transition state[30] are in good agreement with experimental data (Table 4).

Electronic Spectrum of [Ru(bmpie)$_3$].—Besides a few papers on electrochemical properties of Ru^{2+} complexes,[12,31,32] numerous exhaustive studies on the absorption and emission spectra of these compounds have been published.[5,6,8–11,13] We will not discuss the details of the results and the proposed conclusions especially as these studies are concerned with ligands such as pyridine or phenanthroline and not with diazadienes. We have recorded the u.v. and visible absorption spectra of the complexes [Ru(bmpie)$_3$]$^{2+}$ and [Ru(bmpie)$_3$][17] so that they could be compared to our results (obtained by MSXα calculations in the transition state formalism, Table 6). The theoretical results concerning ruthenium(II) were published by Daul and Weber[14] and come from calculations run under conditions comparable to ours.

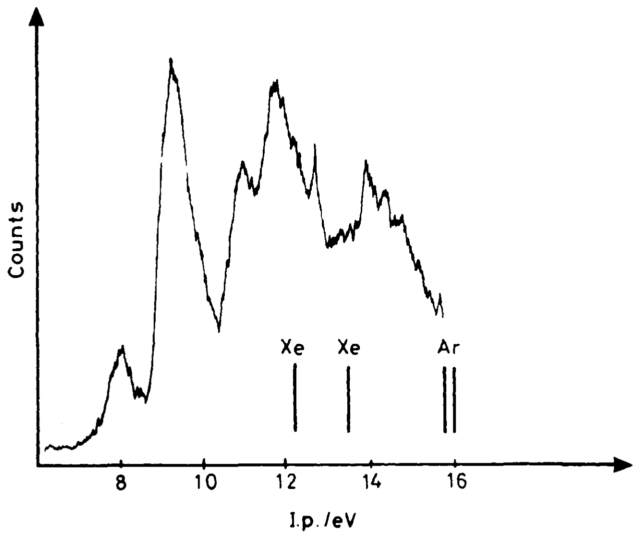

Figure 5. He(I) Photoelectron spectrum of [Ru(bmpie)$_3$]

Theoretically, the calculations take non-polarized spin into account and the theoretical values (nm) are overestimated for

Table 6. Calculated (transition-state procedure) and experimental wavelengths (nm) corresponding to electronic transitions of $[Ru(bmpie)_3]^{2+}$ and $[Ru(bmpie)_3]$

	$[Ru(bmpie)_3]^{2+}$		$[Ru(bmpie)_3]$	
Transition	Exp.	Calc.	Exp.	Calc.
$6a_2 \rightarrow 13e$				4 013
$6a_2 \rightarrow 8a_1$			550	531
$7a_1 \rightarrow 6a_2$	550	518		
$6a_2 \rightarrow 14e$			410	487
$7a_1 \rightarrow 13e$	425	477		463
$12e \rightarrow 6a_2$		447		
$12e \rightarrow 13e$		416		418
$6a_2 \rightarrow 15e$				376
$6a_2 \rightarrow 9a_1$			315	327
$6a_2 \rightarrow 16e$				316
$6a_2 \rightarrow 10a_1$				313
$6a_2 \rightarrow 17e$				311
$11e \rightarrow 13e$				308

singlet–singlet transitions and underestimated for singlet–triplet transitions. Thus, if E_S is the energy of the singlet excited state and E_T the energy of the corresponding triplet state, the calculated energy E is given by the equation below.[33]

$$E = \tfrac{1}{4}(E_S + 3E_T)$$

When considering the experimental results obtained by Ferguson and Herren [13] on the $[Ru(bipy)_3]^{2+}$ ion, the singlet–triplet gap can be roughly estimated as lying between 60 and 90 nm according to the states considered, thus overestimating the singlet state by *ca.* 50 nm and underestimating the triplet states by *ca.* 20 nm. We must of course be very careful with these estimations as the ligands studied here are different.

Absorption spectra of both complexes $[Ru(bmpie)_3]^{2+}$ and $[Ru(bmpie)_3]$ are quite similar. They consist, in the range 300—600 nm, of two very broad bands: the first (relatively weak and broad, ε *ca.* 6 000 dm³ mol⁻¹ cm⁻¹) is at *ca.* 550 nm for Ru^{II} and Ru^0, the other (more intense, ε *ca.* 20 000) is at *ca.* 425 nm for the ion and 410 nm (with a shoulder at 315 nm) for the neutral complex (Table 6). As these bands are very broad (100 nm at half-height for the most intense) we attributed several transitions to each of them (Table 6).

From those calculations the most remarkable feature of $[Ru(bmpie)_3]$ should be the presence for the 20-electron complex of a $6a_2 \rightarrow 13e$ transition (very weak). It should be in the i.r. region between 2 400 and 2 500 cm^{-1} (calculation gives 4 013 nm or 2 492 cm^{-1}). Unfortunately it was not observed under our experimental conditions. Nevertheless, this transition can explain the magnetic behaviour of the complex which varies as a function of temperature.[16,17] Thus, the first excited triplet state ^3E, which should have a paramagnetic character, only requires a low energy (*ca.* 2 400 cm^{-1}) for population; this partly represents the electronic structure of the complex at room temperature whereas at low temperature only the diamagnetic fundamental state is populated. This singlet→triplet temperature-dependent equilibrium related to a small h.o.m.o.–l.u.m.o. separation has already been observed, especially in the case of anthracene and phenanthrene.[34]

Thus, according to this hypothesis, some of the $[Ru(bmpie)_3]$ molecules would be in an excited triplet state at the temperature where the photoelectron spectra are run. It is easy to show that to a first approximation the ionization potentials will hardly vary whether considering the molecule in its fundamental state or in its first excited triplet state. The only exception is the first band which should show a splitting approximately equal to the energy gap between the fundamental and the triplet state (*ca.* 0.3 eV). It is obvious from the shape and low resolution of the spectrum (due to band overlap) that such a splitting could not be observed (Figure 5).

Experimental

Photoelectron spectra were recorded with Perkin-Elmer PS 18 and model 0078 (of PES Laboratories) photoelectron spectrometers and calibrated with $^2P_{\frac{1}{2}}$ and $^2P_{\frac{3}{2}}$ lines of Ar and Xe.

The vapour pressure of the complex was too low for recording the He(II) spectrum.

Acknowledgements

We thank Dr. J. Weber for the loan of the MSXα program, Dr. M. J. L. Garcia for help with the m.o. drawings, and Mrs. F. Gracian for recording the photoelectron spectra.

References

1 Part 18, D. Gonbeau and G. Pfister-Guillouzo, *J. Electron. Spectrosc., Relat. Phenom.*, 1984, **33**, 279.
2 G. Van Koten and K. Vrieze, *Adv. Organomet. Chem.*, 1983, **21**, 178 and refs. therein.
3 J. M. Lehn and J. P. Sauvage, *Nouv. J. Chim.*, 1977, **1**, 449.
4 V. Balzani, F. Bolleta, M. T. Gandolfi, and M. Maestri, *Top. Curr. Chem.*, 1978, **75**, 1.
5 P. Day and N. Sanders, *J. Chem. Soc. A*, 1967, 1536.
6 G. D. Hager and G. A. Grosby, *J. Am. Chem. Soc.*, 1974, **97**, 7031.
7 R. F. Dallinger and W. H. Woodruff, *J. Am. Chem. Soc.*, 1979, **101**, 4391.
8 F. Felix, J. Ferguson, H. U. Güdel, and A. Ludi, *J. Am. Chem. Soc.*, 1980, **102**, 4096.
9 A. Caulemans and L. G. Vanquickenborne, *J. Am. Chem. Soc.*, 1981, **103**, 2238.
10 C. M. Carlin and M. K. De Armond, *Chem. Phys. Lett.*, 1982, **89**, 297.
11 J. Ferguson and F. Herren, *Chem. Phys. Lett.*, 1982, **89**, 371.
12 N. Kitamura, Y. Kawanishi, and S. Tazuke, *Chem. Phys. Lett.*, 1983, **97**, 103.
13 J. Ferguson and F. Herren, *Chem. Phys.*, 1983, **76**, 45.
14 C. A. Daul and J. Weber, *Chem. Phys. Lett.*, 1981, **77**, 593.
15 C. Jung and O. Ristau, *Theor. Chim. Acta*, 1983, **63**, 143.
16 B. Chaudret, H. Köster, and R. Poilblanc, *J. Chem. Soc., Chem. Commun.*, 1981, 266.
17 B. Chaudret, C. Cayret, H. Köster, and R. Poilblanc, *J. Chem. Soc., Dalton Trans.*, 1983, 941.
18 K. H. Johnson, *Adv. Quantum Chem.*, 1973, **7**, 143.
19 J. C. Slater, 'Quantum theory of molecules and solids,' McGraw Hill, New York, 1974.
20 J. B. Danese and J. W. D. Connolly, *J. Chem. Phys.*, 1974, **61**, 3063.
21 R. Hoffmann, *J. Chem. Phys.*, 1963, **39**, 1397.
22 R. Hoffmann and W. N. Lipscomb, *J. Chem. Phys.*, 1962, **36**, 3179, 3489; 1962, **37**, 2872.
23 R. Hoffmann and P. Hofmann, *J. Am. Chem. Soc.*, 1976, **98**, 598.
24 V. I. Baranouskii and A. B. Nikolskii, *Teor. Eksp. Khim.*, 1967, **3**, 527.
25 R. Hoffmann, H. Fujimoto, J. R. Swenson, and C. C. Wan, *J. Am. Chem. Soc.*, 1973, **95**, 7644.
26 M. J. S. Dewar and W. Thiel, *J. Am. Chem. Soc.*, 1977, **99**, 4899, 4907.

27 M. Beez, C. Bieri, H. Bock, and E. Heilbronner, *Helv. Chim. Acta*, 1973, **56**, 1028.

28 D. P. Rillema, D. S. Jones, and H. A. Levy, *J. Chem. Soc., Chem. Commun.*, 1979, 849.

29 S. D. Worley, T. R. Webb, and T. Y. Ou, *J. Electron. Spectrosc. Relat. Phenom.*, 1982, **28**, 129.

30 J. R. Slater, *Adv. Quantum Chem.*, 1972, **6**, 1.

31 N. E. Tokel-Takvoryan, R. E. Hemingway, and A. J. Bard, *J. Am. Chem. Soc.*, 1973, **95**, 6582.

32 A. G. Motten, K. Hanck, and M. K. De Armond, *Chem. Phys. Lett.*, 1981, **79**, 541.

33 P. S. Bagus and B. I. Bennet, *Int. J. Quantum Chem.*, 1975, **9**, 143.

34 A. Minsky, A. Y. Meyer, and M. Rabinovitz, *Angew. Chem., Int. Ed. Engl.*, 1983, **22**, 45.

Received 9th February 1984; *Paper* 4/232